ChemComm

RSC Publishing

COMMUNICATION

View Article Online
View Journal | View Issue

Cite this: *Chem. Commun.*, 2013, **49**, 1963

Received 14th December 2012,
Accepted 18th January 2013

DOI: 10.1039/c3cc38949a

www.rsc.org/chemcomm

Supramolecular polymerization in water harnessing both hydrophobic effects and hydrogen bond formation†

Christianus M. A. Leenders, Lorenzo Albertazzi, Tristan Mes, Marcel M. E. Koenigs, Anja R. A. Palmans* and E. W. Meijer*

The formation of supramolecular polymers in water through rational design of a benzene-1,3,5-tricarboxamide (BTA) motif is presented. Intermolecular hydrogen bonding and hydrophobic effects cooperate in the self-assembly into long fibrillar aggregates. Minimal changes in molecular structure significantly affect the internal packing of the aggregates.

Since the first example of a hydrogen-bonded supramolecular polymer,[1] the field of supramolecular polymer chemistry has become a distinct part of materials research.[2,3] Numerous self-assembling motifs have emerged and detailed studies showed that hydrogen bonding, π–π stacking and metal coordination are the main driving forces for self-assembly in organic solvents.[4,5] In water, however, the hydrophobic effect represents an additional interaction driving self-assembly processes.[6] Assembly of small molecules in water has attracted much interest for several applications. Low molecular weight (LMW) hydrogelators, for example, in most cases rely on the assembly of small molecules into fibrillar structures to immobilize water. Although much progress has been made in recent years,[6–9] it is still difficult if not impossible to predict the assembly and hydrogelation properties of a small molecule from its molecular structure.[10]

In apolar organic solvents, *N*,*N*′,*N*″-trialkyl-benzene-1,3,5-tricarboxamides (BTAs) self-assemble in a cooperative fashion into helical, one-dimensional stacks *via* threefold hydrogen bonding between the amides.[11–13] In view of the importance of water as a solvent for self-assembly processes, we rationally redesigned the BTA motif to become water-compatible. While hydrogen-bond driven self-assembly in water has been reported for several systems,[14–18] only a few examples of supramolecular polymers in water based on the BTA motif have been reported.[19–22] Here, we report on a simple molecular design using merely aliphatic chains to shield a central hydrogen-bonding unit from the surrounding polar media, carrying hydrophilic ethylene glycol motifs in the periphery to ensure solubility (Scheme 1, top). We investigate a series of three water-compatible BTA derivatives **1**–**3** (Scheme 1, bottom). BTA derivative **1** is decorated with aliphatic spacers creating a hydrophobic pocket, and tetraethylene glycol motifs in the periphery with alcohol end groups to provide solubility in water.[23] By introducing a stereogenic center in (*S*)-**2**, the self-assembly can be probed by circular dichroism (CD) spectroscopy, providing information on the helical order within the aggregate.[24] Finally, the amides in BTA derivative **3** are methylated to assess the contribution of intermolecular hydrogen bonding to the self-assembly.

Achiral BTA derivative **1** was obtained *via* a straightforward procedure using protecting group chemistry yielding the alcohol end groups (ESI,† Scheme S1). BTA derivative (*S*)-**2** was synthesized starting from (*S*)-citronellol to introduce a stereogenic methyl side group in the aliphatic spacer (Scheme 1, top).[25] After protection of the alcohol, the double bond was cleaved by ozonolysis. Subsequently, a Wittig reaction was performed to obtain a spacer with a stereogenic methyl group on the third carbon and the protected tetraethylene glycol motif at the other end. In subsequent steps the

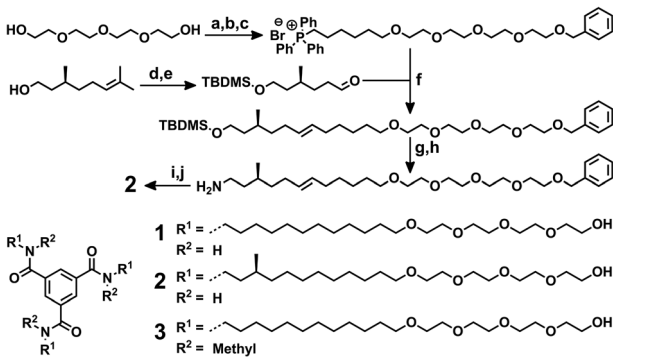

Scheme 1 (top) Synthetic route towards **2**. (a) NaH, THF, 0 °C, benzylbromide, room temperature (RT), overnight, 58%; (b) NaH, THF, 0 °C, 1,6-dibromohexane, RT, overnight, 50%; (c) PPh_3, 140 °C, 7 days, 93%; (d) imidazole, TBDMS chloride, DMF, 0 °C to RT, overnight, quantitative; (e) DCM, O_3(g), −80 °C, DMS, RT, 1 h, 91%; (f) THF, *n*-BuLi, −30 °C, −80 °C to RT, 3 h, 59%; (g) TBAF, THF, 0 °C to RT 4.5 h, 91%; (h) (1) phthalimide, PPh_3, DIAD, ether, 0 °C to RT, overnight. (2) N_2H_4, ethanol, 80 °C, overnight, 81%; (i) 1,3,5-benzenetricarbonyl trichloride, triethylamine, $CHCl_3$, 0 °C to RT, 4 h, 77%; (j) Pd/C, H_2(g), methanol, RT, overnight, 98%. (bottom) Molecular structures of **1**, **2** and **3**.

Institute for Complex Molecular Systems, Eindhoven University of Technology, P.O. Box 513, 5600 MB Eindhoven, The Netherlands. E-mail: e.w.meijer@tue.nl, a.palmans@tue.nl; Fax: +31 (0)40 2451036; Tel: +31 (0)40 2473101

† Electronic supplementary information (ESI) available: Experimental details, characterization by UV and fluorescence spectroscopy and cryo-TEM. See DOI: 10.1039/c3cc38949a

alcohol unit was deprotected and converted into an amine *via* a Gabriel synthesis. After coupling with the aromatic triacid trichloride, the reduction of the double bond and deprotection of the tetraethylene glycol were achieved in one step yielding (*S*)-**2**. Methylation of the core amides of **1** with methyl iodide yielded **3**.

Solutions of **1** in water were prepared by heating **1** in water to temperatures above 80 °C, upon which the mixture became hazy. After cooling to 20 °C, a clear viscous solution was obtained (η_{rel} = 1.43 at $c = 3 \times 10^{-4}$ M), suggesting that **1** indeed forms large aggregates. (*S*)-**2** is less soluble in water, therefore, samples were prepared by injection of methanol into water (ESI†).

In order to study the supramolecular polymerization in detail, the aggregates were visualized by cryo-TEM (Fig. 1; ESI,† Fig. S1). Clearly, both **1** and (*S*)-**2** form long thin fibers in the order of micrometers in length with a diameter of approximately 5 nanometers. The high aspect ratio is an interesting feature of these supramolecular polymers; recent examples of BTA assemblies in water and BTA based hydrogelators were shown to assemble in fibrillar or bundled structures with much larger diameters.[20–22] Interestingly, a close inspection of the aggregates reveals significant differences between the exact packing of the two BTA derivatives (ESI,† Fig. S1). In particular, **1** shows a slightly larger diameter and a subtle and periodic variation in the contrast and diameter, which is not observed in (*S*)-**2**. Such an effect is often observed for helical bundles or twisted ribbons.[7]

To further elucidate the internal packing, the aggregation behaviour of BTAs **1** and (*S*)-**2** was studied by UV-Vis and CD spectroscopy. In organic solvents, a single absorption maximum at 193 nm is indicative of BTA-based helical columnar stacks held together by threefold intermolecular hydrogen bonds, while a maximum at 208 nm is representative of the molecularly dissolved state.[11] In methanol, the UV spectrum of **1** shows an absorption maximum at 209 nm, consistent with the molecularly dissolved state (ESI,† Fig. S2). In water, at 20 °C the UV spectrum of **1** shows two distinct absorption bands at 211 nm and 226 nm (Fig. 2A). Heating the solution from 20 °C to 50 °C does not lead to visible changes in the shape and intensity of the UV spectra. At temperatures above 50 °C, the absorption spectrum gradually changes, resulting in only a single band at 209 nm at 70 °C. The lower critical solution temperature (LCST) of **1** is reached at temperatures above 70 °C (ESI,† Fig. S3) and presents the upper limit for temperature-dependent measurements. Interestingly, the UV spectrum of chiral analogue (*S*)-**2** in water at 20 °C differs significantly from that of **1** and shows an absorption maximum at 192 nm (Fig. 2B), and a Cotton effect at 220 nm ($\Delta\varepsilon = -40$ M^{-1} cm^{-1}), similar to columnar helical stacks of (*S*)-BTAs in organic solvent.[24] In methanol, the absorption spectrum of (*S*)-**2** displays an absorption maximum at 209 nm (ESI,† Fig. S2) and the solution is CD silent, which is consistent with the molecularly dissolved state also observed for **1**. These results suggest that both **1** and (*S*)-**2** self-assemble in water at 20 °C. Aggregates of **1** appear to be stable up to 50 °C and then gradually dissociate reaching a state where all hydrogen bonds are broken at 70 °C. Above 50 °C, also the viscosity decreases, corresponding well to the observed changes in the UV absorption. For (*S*)-**2**, precipitation was observed before a shift in the UV absorption was recorded. The absorption spectra of **1** and (*S*)-**2** suggest that (*S*)-**2** adopts the reported helical columnar packing, while **1** adopts a different packing within the supramolecular polymer, consistent with the cryo-TEM results. The details of the packing of **1**, however, remain unclear. This indicates that the minimal difference in the hydrophobic chains of **1** and (*S*)-**2** has a dramatic effect on the packing of the monomers resulting in different fibrillar structures.

Intrigued by the difference in packing between aggregates of **1** and **2**, the aggregation of **1** was studied as a function of time (Fig. 2C). A small volume of a concentrated solution of **1** in methanol was injected into water (final concentration $c = 1 \times 10^{-5}$ M) and the UV absorption spectrum was recorded at set intervals. Directly after injection the absorption spectrum displays a maximum at 192 nm, as was observed for (*S*)-**2**. In time, however, the absorption spectrum undergoes a red shift *via* an isosbestic point. The absorption maximum at 192 nm suggests that initially helical, columnar, one-dimensional stacks are formed that subsequently convert

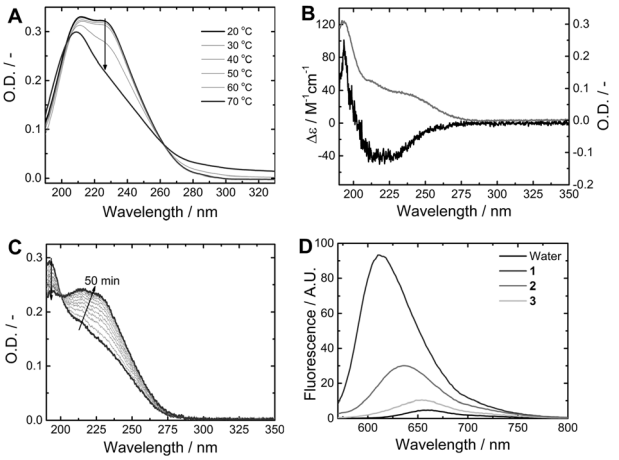

Fig. 2 (A) UV-Vis absorption of **1** ($c = 1 \times 10^{-5}$ M) in water, as a function of temperature (the arrow indicates the trend upon heating). (B) UV-Vis absorption (grey) and CD (black) spectra of **2** ($c = 1 \times 10^{-5}$ M) in water. (C) Evolution of UV-Vis absorption of **1** ($c = 1 \times 10^{-5}$ M) in water (the arrow indicates trend in time). (D) Nile Red fluorescence in pure water (black), solution of **1** (dark grey), **2** (grey) or **3** (light grey) ($c = 1 \times 10^{-5}$ M).

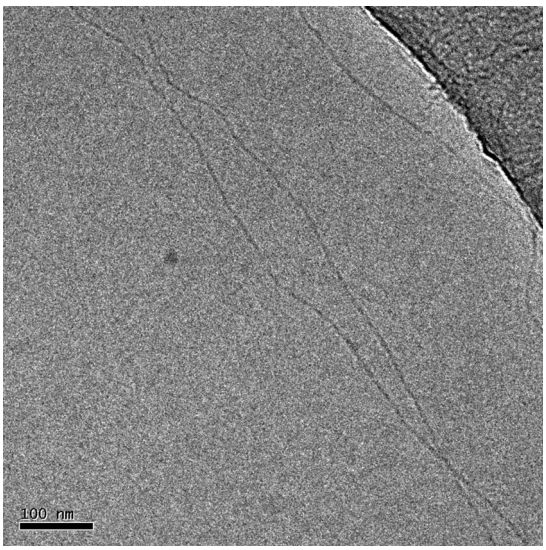

Fig. 1 Cryo-TEM image of **1** in water, showing long very narrow fibrillar aggregates. Scale bar represents 100 nm.

into the structures observed by cryo-TEM. In contrast, for solutions of (*S*)-**2** in water, no transition occurs in time after injection of methanol, which suggests that (*S*)-**2** is in the thermodynamically stable state. Possibly, the stereogenic methyl side group in (*S*)-**2** preorganizes the molecules resulting in a preference for a columnar packing.

These observations stress the importance of a careful design of the aliphatic spacers. However, the contribution of intermolecular hydrogen bonds to the stabilisation of the aggregates remains unclear. Therefore, we assessed the presence of hydrogen bonding in the aggregates of **1** in water by the addition of hexafluoroisopropanol (HFIP), a denaturant that is capable of interfering with intermolecular hydrogen bonds.[16] Upon addition of small aliquots of HFIP to a solution of **1** in water (ESI,† Fig. S4) the absorption maximum gradually shifts to lower wavelengths, indicating depolymerization of the aggregates. The changes in the UV spectra upon addition of HFIP are comparable to those observed upon increasing the temperature. As such, it is likely that hydrogen bonds play an important role in the stabilisation of the aggregates of **1** and (*S*)-**2**.

Additional proof for the importance of the hydrogen bonds in the aggregate formation was obtained by methylation of the BTA amide groups in **3**. As a result, **3** cannot form intermolecular hydrogen bonds[26] and the potential aggregation of **3** can only be the result of its amphiphilic nature. The aggregation behaviour of **3** in water and methanol was studied by UV-Vis spectroscopy. The UV spectrum of **3** does not change upon changing the solvent from water to methanol (ESI,† Fig. S6). These results show that **3** does not form supramolecular polymers in either one of the solvents at the applied concentration, indicating the importance of hydrogen bonding for aggregate stabilization.

After studying the significance of intermolecular hydrogen bond formation, the contribution of hydrophobic effects to the self-assembly process was selectively assayed by probing the polarity of the hydrophobic pocket using the solvatochromic dye Nile Red. In pure water Nile Red displays low fluorescence intensity, which increases in more apolar solvents. Furthermore, the fluorescence wavelength depends on the polarity of the environment. This tool has been widely used to probe the formation of self-assembled structures with a hydrophobic core.[27]

Self-assembly of BTA molecules in water will result in a strong enhancement of fluorescent intensity due to probe encapsulation and the emission wavelength will provide information about the polarity of the hydrophobic pocket.[16] Compared to pure water, the fluorescence intensity of Nile Red in a solution of **1** increases by two orders of magnitude and a large blue shift is observed (Fig. 2D). Interestingly, in a solution of (*S*)-**2**, the blue shift is smaller and the fluorescence intensity is lower. Furthermore, compound **3** shows almost no difference compared to pure water, and only at higher concentration ($c = 5 \times 10^{-5}$ M) a blue shift and increase in intensity is observed (ESI,† Fig. S7), indicating that the initial concentration is below the critical aggregation concentration. The difference in fluorescence wavelength and intensity confirms that **1** and (*S*)-**2** adopt a different packing within the aggregates. The packing of **1** results in the formation of a more apolar hydrophobic domain, even though it has fewer carbons in the spacer. The low fluorescence increase of **3** further supports the importance of stabilization of the aggregates by hydrogen bonding.

In summary, we have rationally designed several water-soluble BTA derivatives and studied their self-assembly in water. These molecules self-assemble into supramolecular polymers, micrometers in length and only a few nanometers in diameter. UV-Vis and fluorescence spectroscopy supports that both hydrophobic effects and hydrogen bonding play a crucial role in the formation of these fibrillar aggregates. These results highlight the potential of combining hydrogen bonding and hydrophobic effects for the formation of supramolecular polymers in water and contribute to the development of general guidelines for the rational formation of one-dimensional assemblies in water.

Notes and references

1 C. Fouquey, J.-M. Lehn and A.-M. Levelut, *Adv. Mater.*, 1990, **2**, 254–257.
2 T. Aida, E. W. Meijer and S. I. Stupp, *Science*, 2012, **335**, 813–817.
3 A. Bertrand, F. Lortie and J. Bernard, *Macromol. Rapid Commun.*, 2012, **33**, 2062–2091.
4 L. Brunsveld, B. J. B. Folmer, E. W. Meijer and R. P. Sijbesma, *Chem. Rev.*, 2001, **101**, 4071–4097.
5 X. Yan, F. Wang, B. Zheng and F. Huang, *Chem. Soc. Rev.*, 2012, **41**, 6042–6065.
6 T. Rehm and C. Schmuck, *Chem. Commun.*, 2008, 801–813.
7 L. A. Estroff and A. D. Hamilton, *Chem. Rev.*, 2004, **104**, 1201–1217.
8 M. de Loos, J. H. van Esch, R. M. Kellogg and B. L. Feringa, *Tetrahedron*, 2007, **63**, 7285–7301.
9 Y. Yan, Y. Lin, Y. Qiao and J. Huang, *Soft Matter*, 2011, **7**, 6385–6398.
10 J. H. van Esch, *Langmuir*, 2009, **25**, 8392–8394.
11 M. M. J. Smulders, A. P. H. J. Schenning and E. W. Meijer, *J. Am. Chem. Soc.*, 2008, **130**, 606–611.
12 S. Cantekin, T. F. A. de Greef and A. R. A. Palmans, *Chem. Soc. Rev.*, 2012, **41**, 6125–6137.
13 P. J. M. Stals, M. M. J. Smulders, R. Martin-Rapun, A. R. A. Palmans and E. W. Meijer, *Chem.–Eur. J.*, 2009, **15**, 2071–2080.
14 E. Obert, M. Bellot, L. Bouteiller, F. Andrioletti, C. Lehen-Ferrenbach and F. Boue, *J. Am. Chem. Soc.*, 2007, **129**, 15601–15605.
15 N. Chebotareva, P. H. H. Bomans, P. M. Frederik, N. Sommerdijk and R. P. Sijbesma, *Chem. Commun.*, 2005, 4967–4969.
16 J. Boekhoven, A. M. Brizard, P. van Rijn, M. C. A. Stuart, R. Eelkema and J. H. van Esch, *Angew. Chem., Int. Ed.*, 2011, **50**, 12285–12289.
17 P. Y. W. Dankers, T. M. Hermans, T. W. Baughman, Y. Kamikawa, R. E. Kieltyka, M. M. C. Bastings, H. M. Janssen, N. A. J. M. Sommerdijk, A. Larsen, M. J. A. van Luyn, A. W. Bosman, E. R. Popa, G. Fytas and E. W. Meijer, *Adv. Mater.*, 2012, **24**, 2703–2709.
18 J. D. Hartgerink, E. Beniash and S. I. Stupp, *Science*, 2001, **294**, 1684–1688.
19 P. Besenius, G. Portale, P. H. H. Bomans, H. M. Janssen, A. R. A. Palmans and E. W. Meijer, *Proc. Natl. Acad. Sci. U. S. A.*, 2010, **107**, 17888–17893.
20 S. Lee, J.-S. Lee, C. H. Lee, Y.-S. Jung and J.-M. Kim, *Langmuir*, 2011, **27**, 1560–1564.
21 A. Bernet, R. Q. Albuquerque, M. Behr, S. T. Hoffmann and H.-W. Schmidt, *Soft Matter*, 2012, **8**, 66–69.
22 R. C. T. Howe, A. P. Smalley, A. P. M. Guttenplan, M. W. R. Doggett, M. D. Eddleston, J. C. Tan and G. O. Lloyd, *Chem. Commun.*, 2013, DOI: 10.1039/C2CC37428E.
23 E. E. Dormidontova, *Macromolecules*, 2004, **37**, 7747–7761.
24 Y. Nakano, T. Hirose, P. J. M. Stals, E. W. Meijer and A. R. A. Palmans, *Chem. Sci.*, 2012, **3**, 148–155.
25 E. J. Lenardao, G. V. Botteselle, F. de Azambuja, G. Perin and R. G. Jacob, *Tetrahedron*, 2007, **63**, 6671–6712.
26 M. M. J. Smulders, M. M. L. Nieuwenhuizen, M. Grossman, I. A. W. Filot, C. C. Lee, T. F. A. de Greef, A. P. H. J. Schenning, A. R. A. Palmans and E. W. Meijer, *Macromolecules*, 2011, **44**, 6581–6587.
27 M. C. A. Stuart, J. C. van de Pas and J. B. F. N. Engberts, *J. Phys. Org. Chem.*, 2005, **18**, 929–934.